Characterization of microphone placement and noise sensitivity in a global active noise control system for a compact noise source

Ryan L. Rust[a], Scott D. Sommerfeldt[b], Kent L. Gee[c] and Jonathan D. Blotter[d]

(Received: 19 July 2011; Revised: 27 July 2012; Accepted: 16 April 2013)

This paper presents a sensitivity analysis to error microphone placement and extraneous noise sources for two control source configurations used for the active control of noise radiated from a compact source. The two control configurations analyzed are a linear array of four control sources with the primary source in the middle of the array and a symmetric array of four control sources surrounding the primary source. For modeling purposes, the primary source and the control sources are modeled as simple sources with a baffled free space Green's function to predict the noise measured by the four error microphones. The control source strengths which minimize the squared pressure at the error microphones are solved for based on error microphone locations. If the microphones are placed properly with no error in spatial location, this minimization process has been previously shown to result in radiated power minimization. Simulation results show the linear array is significantly more sensitive to microphone placement errors than the symmetric array. The linear array configuration is also shown to be more sensitive to added random noise in the error signals. Experimental results suggest that for the configurations used, the sensitivity to microphone placement errors was the dominant effect. The reduction in performance for the linear array configuration is significant with microphone placement errors and/or added random noise, while the reduction in performance for the symmetric array is minimal.

Primary subject classification: 38.2; Secondary subject classification: 11.4.1

1 INTRODUCTION

The motivation for the work presented in this paper is connected with previous work investigating the active control of small axial cooling fans, which can be characterized as compact acoustic sources. Active noise control of axial cooling fans has been studied using various control source configurations[1–8]. The range of control system configurations includes simple single control source configurations[1–3] to four control sources in various configurations[5–7]. Gee and Sommerfeldt[5,6] and Monson et al.[7] applied a sound power reduction technique to an axial cooling fan surrounded by symmetrically-arranged loudspeakers. The sound power reduction technique was proposed by Nelson et al.[9] and Elliot et al.[10] to globally attenuate simple noise sources. The global control can be achieved by introducing control sources that are closely spaced to the primary source relative to an acoustic wavelength. Theoretically, optimal control source strengths were found by the minimization of the power radiated by the system of primary and secondary sources. In applying this technique to cooling fans, Gee and Sommerfeldt[5,6] found the optimal near-field error microphone locations by a) modeling all sources as monopoles, b) using the Nelson et al.[9] and Elliott et al.[10] method to theoretically minimize the radiated power, and c) finding where the calculated near-field pressure level reduction was the greatest. By then placing microphones at those near-field locations of greatest pressure level reduction, it was postulated that minimization of the radiated sound power can be achieved by minimizing the pressure at the near-field sensors. These near-field locations where pressure level reduction is greatest when minimizing the radiate power will be referred to as the optimal locations. However, because minimization of the

[a] Brigham Young University, 435 Crabtree Building, Provo, UT 84602 USA; email: ryrust@gmail.com.
[b] Brigham Young University, N181 Eyring Science Center, Provo, UT 84602 USA; email: scott_sommerfeldt@byu.edu.
[c] Brigham Young University, 435 Crabtree Building, Provo, UT 84602 USA; email: kentgee@byu.edu.
[d] Brigham Young University, 435 Crabtree Building, Provo, UT 84602 USA; email: jblotter@byu.edu

squared-pressure at discrete locations does not necessarily guarantee the source coupling that will result in minimized radiated power, near-field measurements were used to confirm the validity of this approach[11].

Optimization of active control systems has also been a source of emphasis, including the optimal placement of error sensors and control source placement[12–19]. For instance, Clark and Fuller[12] used an algorithm to optimize the placement of a piezoelectric actuator and strain error sensor to control the sound radiated from a baffled simply supported plate. Berkhoff[13] found that there was an optimal distance between control sources and error sensors for the active control of sound transmission through a plate. Pulthasthan and Pota[14] used an energy based approach to find the optimal actuator and sensor locations to control structural radiation. Additionally, genetic algorithms have also been implemented to find the optimal locations for control sources and error sensors. In research designed to optimize attenuation of noise from axial cooling fans, Duke et al.[16] used a genetic algorithm to investigate the control of compact noise sources and improve upon the symmetric four control source arrangement used by Gee and Sommerfeldt[5,6]. The genetic algorithm results showed that including the primary source within a linear array of four control sources, two on each side of the primary source, was the optimal control source configuration that minimized the sound power of the primary source. Experiments showed improved performance relative to Gee and Sommerfeldt's symmetric source arrangement. However, Duke et al.[16] were not able to achieve the theoretical reductions in radiated power predicted from the linear array of sources. The fact that the linear array configuration was unable to achieve the theoretical attenuations suggested that other aspects of the control system were limiting the attenuation. Hansen and Snyder[20] proposed that a number of different aspects of an active control configuration impact the attenuation achieved in addition to control source configuration, including error sensor placement, quality of the reference signal and the controller.

When implementing active noise control in previous research, the acoustic pressure was minimized at the error sensors (typically using the filtered-x algorithm). However, minimization of the acoustic pressure did not always result in achievement of the predicted reduction in radiated power, even though the pressure at the error sensors was generally reduced down to the noise floor. The aim in this paper was to find the impact of the error sensor placement on the control system by simulating the control configuration used by Duke et al.[16] compared to the symmetric control system used by Gee and Sommerfeldt[5,6]. It will be shown that in some configurations, if the placement of the error sensors varies even a small amount from the optimal locations, significant degradation of the performance will occur.

2 EFFECTS OF SPATIAL ERRORS

The control approach adopted in this work relies on placing one or more error sensors in the near field of the sources, which has the effect of creating a nodal line at the location of the sensors. This concept will be reviewed briefly for the case of two point sources located a distance d apart, which will aid in understanding the effect of placing the error sensors at suboptimal locations.

Consider a primary point source with source strength, Q_p, placed on the positive x-axis a distance x_0 from the origin. A secondary point source with complex source strength, $Ae^{j\phi}$, is placed on the negative x-axis, also a distance x_0 from the origin. The complex pressure field response can then be expressed as

$$p = \frac{j\rho ckQ_p}{4\pi r_1} e^{-jkr_1} + \frac{j\rho ckAe^{j\phi}}{4\pi r_2} e^{-jkr_2}, \qquad (1)$$

where ρ is the fluid density, c is the speed of sound, k is the acoustic wavenumber, and r_1 and r_2 are the distances from the primary and secondary control sources to the field point, respectively.

For a dipole, $A = Q_p$ and $\phi = \pi$. When this solution is implemented, a nodal plane is created on the y–z plane at $x = 0$. This solution can also be obtained by placing an error sensor in this plane and having the control system drive the pressure at the error sensor to zero. It turns out that this is not the solution that minimizes the radiated acoustic power. As shown by Nelson and Elliott[21], the optimal solution for minimizing radiated power is for $A = sinc(kd)$ and $N = \pi$. When this solution is implemented, a nodal plane is again created, but it is not at $x = 0$. For the specific parameters of $x_0 = 0.03$ m and a frequency of 600 Hz the pressure nodal plane is shifted towards the secondary control source by about 1 mm. For these parameters, the radiated power is attenuated by 8.4 dB using the dipole solution, and by 8.6 dB using the optimal solution. Thus, while this is not a large difference for this case, by shifting the location of the error sensor by about 1 mm one would expect a change of about 0.2 dB in the acoustic power that is radiated.

Continuing this example, we can implement a control source strength that will minimize the squared pressure at any location along the line between the two sources. This source strength is given by

$$Ae^{j\emptyset} = \frac{r_2}{r_1} Q_p. \qquad (2)$$

For a given source strength, the radiated power can be expressed as

$$\Pi = \Pi_p\left[1 + A^2 + 2Asinc\,(kd)\cos(\phi)\right], \qquad (3)$$

where Π_p is the power radiated by the primary source with no control. The power that is radiated as a function of sensor location is shown in Fig. 1, where it can be seen that minimizing the pressure at a suboptimal location in the near field will reduce the level of power attenuation that can be achieved by the control system.

While the changes in radiated power are not dramatic for small errors in error sensor location in this simple example, for complex higher order sources such as are investigated in this article, the effects can become much more significant. It will be shown that for some control configurations, even small errors in placing the error sensors can yield significant changes in the attenuation of the radiated sound power that can be achieved.

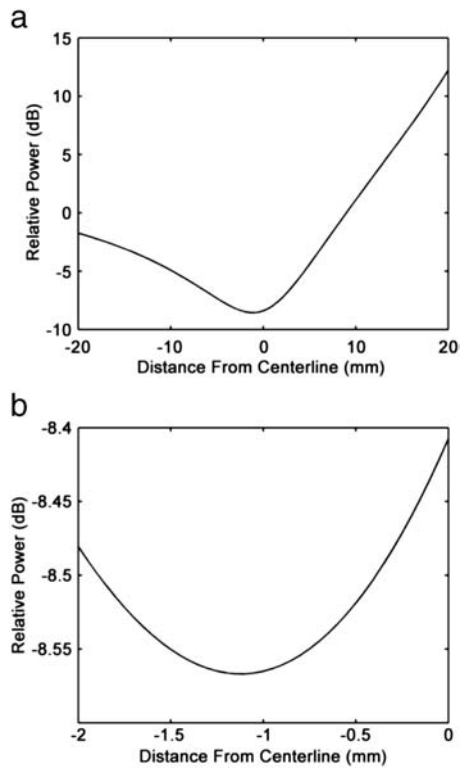

Fig. 1—Attenuation of the radiated power as a function of error sensor location along the line joining the primary source and the secondary control source. a) Error sensor moved through the range of 20 mm to either side of the centerline between the sources, and b) Zoomed in to show the optimal location approximately 1.1 mm off the centerline (negative distance is towards the secondary control source).

3 SIMULATION

3.1 Global Active Control

A brief overview of the free field active noise control theory developed by Nelson and Elliott[21] is presented in this section as the basis for the simulation of the control system. Free field global active noise control uses near field control sources that are closely spaced relative to a wavelength to minimize the sound power of a primary source. Each source contributes to the overall sound power and creates a radiation impedance between itself and all sources present according to

$$Z(kd) = \frac{jk^2\rho_o c}{4\pi}\left(\frac{e^{-jkd}}{kd}\right), \qquad (4)$$

where k is the wave number, d is the distance between the two sources, ρ_o and c are the density and speed of sound in the medium respectively. (The so-called self-impedance occurs when $d \to 0$.) Using Eqn. (4), impedance matrices can then be constructed to find the total sound power of a configuration of sources. The matrix $\overline{\boldsymbol{Z}}_{cc}$ can be defined as a control source impedance matrix between all of the control sources. Additionally, the primary source impedance matrix, $\overline{\boldsymbol{Z}}_{pp}$, includes elements representing the impedances between all primary sources. Lastly, $\overline{\boldsymbol{Z}}_{cp}$ and $\overline{\boldsymbol{Z}}_{pc}$ are matrices with impedances coupling the primary and secondary sources, where $\overline{\boldsymbol{Z}}_{cp} = \overline{\boldsymbol{Z}}_{pc}^{T}$. Using these impedance matrices to break up the sound power expression into control and primary sources, the total sound power is given by,

$$\Pi = \frac{1}{2}\Big(\overline{\boldsymbol{Q}}_p^H Re\left[\overline{\boldsymbol{Z}}_{pp}\right]\overline{\boldsymbol{Q}}_p + \overline{\boldsymbol{Q}}_c^H Re\left[\overline{\boldsymbol{Z}}_{pc}\right]\overline{\boldsymbol{Q}}_p + \overline{\boldsymbol{Q}}_p^H Re\left[\overline{\boldsymbol{Z}}_{cp}\right]\overline{\boldsymbol{Q}}_c + \overline{\boldsymbol{Q}}_c^H Re\left[\overline{\boldsymbol{Z}}_{cc}\right]\overline{\boldsymbol{Q}}_c\Big) \qquad (5)$$

where $\overline{\boldsymbol{Q}}_c$ is the complex control source strength vector, whose elements are the control source strengths of each control source, $\overline{\boldsymbol{Q}}_p$ is the complex source strength vector of the primary sources, and H is the Hermitian transpose. Defining

$$\overline{\boldsymbol{A}} = \frac{1}{2}Re\left[\overline{\boldsymbol{Z}}_{cc}\right], \qquad (6)$$

$$\overline{\boldsymbol{B}} = \frac{1}{2}Re\left[\overline{\boldsymbol{Z}}_{pc}\right], \overline{\boldsymbol{Q}}_p, \qquad (7)$$

$$C = \frac{1}{2}\overline{\boldsymbol{Q}}_p^H Re\left[\overline{\boldsymbol{Z}}_{pp}\right], \overline{\boldsymbol{Q}}_p, \qquad (8)$$

simplifies the sound power expression. By minimizing the sound power expression with respect to the

control source strength vector, the optimal control source strengths are determined to be,

$$\overline{\boldsymbol{Q}}_{so} = -\,\overline{\boldsymbol{A}}^{-1}\,\overline{\boldsymbol{B}}, \tag{9}$$

with the minimized sound power given as

$$\Pi_{min} = C - \,\overline{\boldsymbol{B}}^{H}\,\overline{\boldsymbol{A}}^{-1}\,\overline{\boldsymbol{B}}. \tag{10}$$

When applying the sound power minimization to a primary source using active noise control, the aim is to have the control configuration achieve the minimized sound power given in Eqn. (10). This approach was implemented with exhaust-mounted cooling fans by Gee and Sommerfeldt,[5,6] Monson et al.[7] and Shafer et al.[11] by modeling the baffled fan and control speakers as simple sources. The optimal control source strengths that minimize the sound power were calculated, and used to predict the near-field controlled pressure field relative to the primary pressure field. The relative pressure field was then used as an error sensor placement map with contours of maximum attenuation being the ideal locations for the error sensors. Using this method, the blade passage frequency and the harmonics of an axial cooling fan were actively controlled. Shafer et al.[11] were able to confirm that the predicted near-field pressure field relative to the primary field was achieved experimentally through using this approach[11].

To optimize the control source configuration, Duke et al.[16] used a genetic algorithm. The algorithm iterated through control source configurations to converge onto the optimal control source locations which minimized the overall sound power. The resulting control source configuration is shown in Fig. 2[16] compared to a symmetric surrounding configuration used by Gee and Sommerfeldt[5,6]. The linear array configuration predicted a reduction in the sound power of 58, 33 and 18 dB at 550, 1100, and 1650 Hz respectively. However, experimental results only achieved 32, 23 and 3 dB[16]. One possible reason for the discrepancy in performance was errors in the placement of the error sensors, which is the focus of this work. It will be emphasized here that the objective of the control system used here is to minimize overall radiated acoustic power, but the controller attempts to do so by minimizing the acoustic pressure at strategically chosen locations. Thus, any error in placing the error sensors at the optimal locations can potentially affect the attenuation of radiated power that can be achieved.

3.2 Control System Modeling

In order to investigate the impact on control performance of error sensor location and extraneous noise in the error signals, a control system model was created and used to test the control configurations under different scenarios. The model allows for the control system performance to be analyzed under different error sensor position combinations. The model is based on representing the control sources as baffled simple sources and the microphones as point sensors. The free space Green's function for a baffled monopole source is used to model the transfer function between the simple sources and the point microphones, given by

$$G = \frac{j\rho_o ck}{2\pi D} e^{-jkD}, \tag{11}$$

where D is the distance between the source and the point of interest in space. The pressure due to the specific source at the chosen point is found by multiplying Eqn. (11) by the source strength, q_s. The total pressure at point m in space can then be calculated using the Green's function between each primary or control source and point m given by

$$p_m = q_1 G_{1m} + q_2 G_{2m} + \cdots + q_n G_{nm}, \tag{12}$$

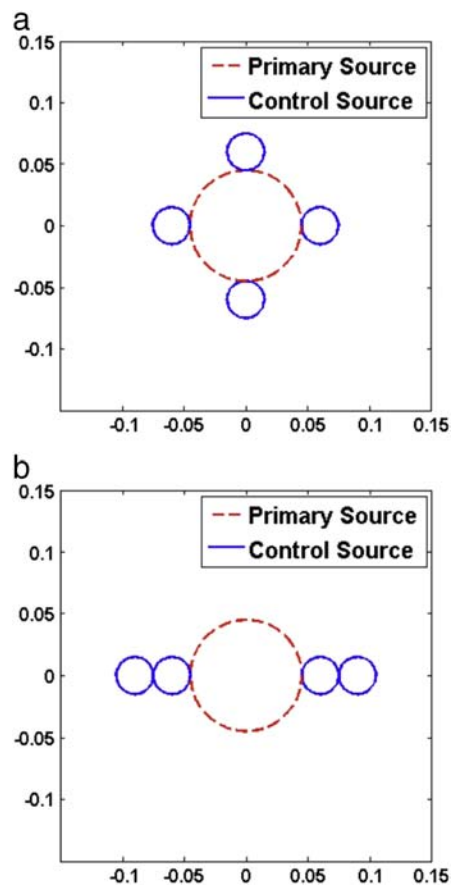

Fig. 2—a) A symmetric configuration of control and primary sources employed by Gee et al.[5,6] b) A linear array of control sources implemented by Duke et al.[16] for use in global active noise control.

where G_{1m} is the Green's function associated with source 1 and point m. Equation (12) can now be used to find the pressure at each error microphone. The pressure of each microphone location is placed into an Mx1 vector, $\bar{P}$, whose elements are found by using Eqn. (12). Separating the control and primary sources in the configuration results in:

$$\bar{P} = \bar{G}_{cc}\,\bar{Q}_c + \bar{G}_{pp}\,\bar{Q}_p, \tag{13}$$

where $\bar{G}_{cc}$ is a matrix of Green's functions from each control source to each of the microphones and $\bar{G}_{pp}$ is a matrix of Green's functions from each primary source to each microphone. In order to simulate the control system, the sum of the squared pressures at each microphone location is found by forming $\bar{P}^H\,\bar{P}$ which results in

$$\begin{aligned}\bar{P}^H\,\bar{P} = {} & \bar{Q}_c^H\,\bar{G}_{cc}^H\,\bar{G}_{cc}\,\bar{Q}_c + \bar{Q}_c^H\,\bar{G}_{cc}^H\,\bar{G}_{pp}\,\bar{Q}_p \\ & + \bar{Q}_p^H\,\bar{G}_{pp}^H\,\bar{G}_{cc}\,\bar{Q}_c + \bar{Q}_p^H\,\bar{G}_{pp}^H\,\bar{G}_{pp}\,\bar{Q}_p.\end{aligned} \tag{14}$$

The sum of the squared pressures at the microphones is minimized in the manner of an active noise control system by taking the derivative of Eqn. (14) with respect to $\bar{Q}_c$ to yield

$$\frac{\partial \bar{P}^H\,\bar{P}}{\partial \bar{Q}_c} = 2\,\bar{G}_{cc}^H\,\bar{G}_{cc}\,\bar{Q}_c + 2\,\bar{G}_{cc}^H\,\bar{G}_{pp}\,\bar{Q}_p. \tag{15}$$

The derivative is set to zero and the control source strengths are solved for, resulting in

$$\bar{Q}_c = -\left(\bar{G}_{cc}^H\,\bar{G}_{cc}\right)^{-1}\left(\bar{G}_{cc}^H\,\bar{G}_{pp}\,\bar{Q}_p\right). \tag{16}$$

Equation (16) gives the source strengths the control system will converge to with the microphones in any configuration. These control source strengths are then used to find the sound power of the control system configuration using Eqn. (5). When the microphones are in the optimal locations, the control source strengths calculated from Eqn. (16) will match Eqn. (9). For a given configuration, the control source strengths in Eqn. (16) are used to calculate the attenuation of the primary source field. Thus, by using this model, the attenuation achieved by a control system can be found as a function of the microphone positions.

3.3 Control System Simulation

The outlined model is used to simulate the two control configurations shown in Fig. 2, i.e. the optimized linear array of control sources and the symmetric configuration. With the microphones in the optimal locations, Shafer et al.[11] confirmed that the near-field controlled pressure relative to the primary pressure was created by the control system for the symmetric configuration. Building upon Shafer's work, the sound power of a primary source operating at 600 Hz was simulated with the two different control configurations. For the simulation, the error microphones were placed in the optimal locations found by Gee et al.[5–7,11], which results in a maximum attenuation of 58 dB for the linear array and 29 dB for the symmetric configuration.

After confirming the control configurations could achieve the predicted maxima, the simulation was then used to investigate the sensitivity of the two control systems relative to microphone placement error. In the simulation, a single microphone was moved with the other three of the four microphones remaining in their optimal locations. The single microphone is moved along a line in space which crosses the optimal location. The movement path of the microphone and the optimal near-field controlled pressure relative to the primary field for both configurations are shown in Fig. 3. A total of three error microphone simulations are performed, one for the symmetric case, and since the linear array has two speakers closer to and two farther from the primary source, two different microphone paths were simulated. All the paths start 1 cm from the optimal location and move 1 cm past the optimal placement, with a total movement of 2 cm per simulation.

Figure 4 shows the results of the single microphone placement error simulation, with distance on the abscissa corresponding to the distance from the ideal placement, with the positive values being further from the primary source. For the two linear configuration microphone placement plots, there is a large, narrow peak in the predicted attenuation, creating a wide range of possible sound power attenuations for small errors in microphone placement. The microphone closer to the primary source leads to attenuation variations from 15–60 dB, while the predicted attenuation for the microphone farther from the primary source varies from 19–60 dB for the 2 cm simulation. Additionally, the peak in the attenuation is narrow for the linear configuration, meaning a microphone placement error of just 2 mm from the ideal placement means a 20–28 dB drop in sound power attenuation. In contrast, the symmetric configuration varies from 20–30 dB across the 2 cm simulation, which is a relatively small range compared to the linear configuration. In particular, a 2 mm error in placement of one microphone from the ideal placement only yields a 0.8 dB decrease in attenuation compared to the large decrease of 20–28 dB for the linear array control configuration. This illustrates that even a small error in sensor placement could account for nearly all of the discrepancy in performance observed by Duke et al.[16]

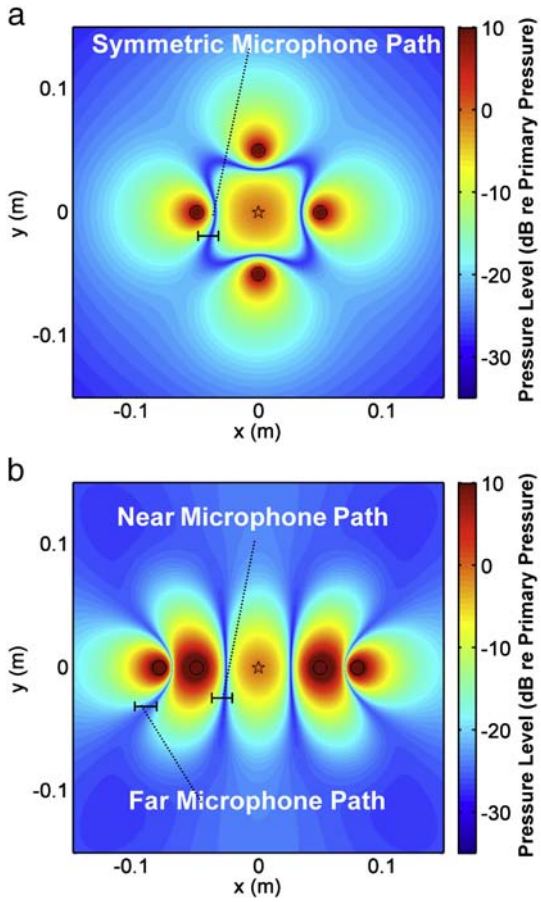

Fig. 3—a) Optimal near-field controlled pressure field relative to the primary field (in dB) for the symmetric configuration of control sources, with the circles as control sources and the star as the primary source. The microphone path used for the non-fixed microphone is shown as the line that crosses the contour of maximum attenuation. b) Optimal near-field controlled pressure field relative to the primary field (in dB) for the linear configuration of control sources, with the circles as control sources and the star as the primary source. The microphone path used for the non-fixed microphone is shown as the line that crosses the contour of maximum attenuation. The linear configuration has two simulations, one for the close microphone path and one for the far microphone path.

Since these control systems use four microphones, the above simulation was repeated incorporating position errors for all of the microphones. As before, one of the four microphones was moved along the same line in space, as shown in Fig. 3, for all three simulations. This microphone is referred to as the simulation microphone. The other three error microphones were given a placement error corresponding to a point on a grid with overall size of 1 mm × 1 mm. This grid was centered on the ideal microphone location, and was broken up into 81 different positions — 9 in each direction. At each increment of the simulation microphone, the other three microphones were individually incremented across their grids to give a total of 531,441 microphone position combinations. The attenuation was calculated for all these microphone position combinations with the maximum and minimum attenuation being saved at each increment of the simulation microphone. The maximum and minimum attenuations give an extreme range of expected values from the control system based on 1 mm error in placement of all the microphones. The results are plotted in Fig. 5, along with the curves from the previous single microphone placement error simulations for all three simulation paths. Figures 5(a) and 5(b) indicate a large variability in possible attenuation values for the linear array configuration. Specifically, when the simulation microphone is near the optimal location, where the horizontal axis is close to zero, the variability in attenuation has a range of 22–23 dB for the linear array control configuration. The large range shows how sensitive the linear configuration is to microphone position errors, especially compared to the 0.4 dB range of variability for the symmetric case [Fig. 5(c)]. Looking further into the two linear array configuration simulations, there is more variability associated with the far microphone than with the near microphone. Specifically, the far microphone has a 23 dB spread at the ideal

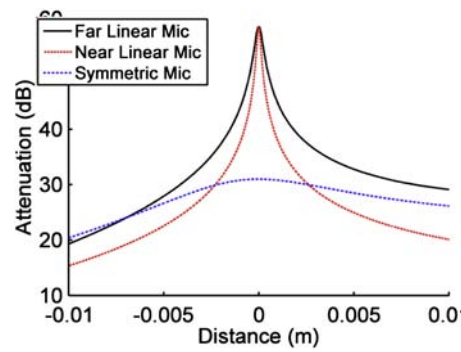

Fig. 4—The simulated sound power attenuation (in dB) for three simulations. One microphone is moved along the paths shown in Fig. 3 while keeping the other microphones stationary, with the abscissa being the distance from the optimal microphone position.

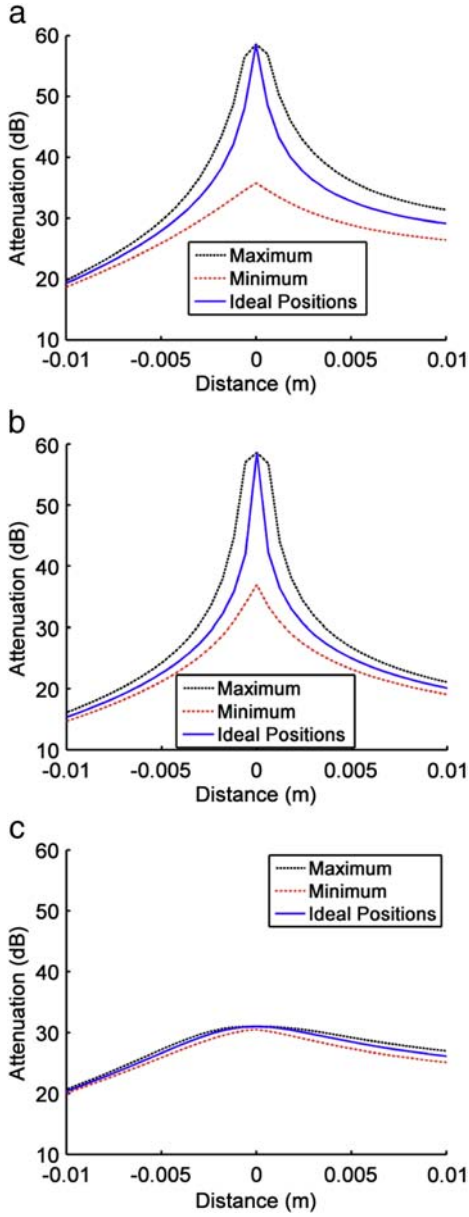

Fig. 5—The simulated sound power attenuation for moving one microphone across the paths shown in Fig. 3 and the other three microphones having position errors in the x and the y direction of 1 mm. The maximum and minimum sound power attenuation curves correspond to the extreme results obtained from the simulations for the a) far microphone moved in the linear configuration, b) near microphone moved in the linear configuration, and c) microphone moved in the symmetric configuration.

placement position compared to a 22 dB range for the near microphone. Additionally, when the simulation microphone was past the optimal location, i.e., farther from the primary source, there is a 5 dB spread in the attenuation for the far microphone compared to a 2 dB spread for the near microphone. The results show that the sensitivity of the linear array control system configuration to microphone placement errors is much greater than that of the symmetric control system configuration.

Moving on from the placement error simulations, the effect of having an area sensor instead of a point sensor is investigated. The sharp peak in predicted attenuation for the linear array configuration because of placement error suggested that the microphone diaphragm size might have an impact on performance of the control system. Thus, the model was changed from having point sensors to area sensors. The free space Green's function was modified to include a surface integral of the pressure across each microphone diaphragm, with an area of 5 mm by 5 mm for each diaphragm. The same process was used to solve for the control source strengths and the resulting sound power with the modified Green's functions, as previously presented. Performing the simulation with all four microphones in the ideal locations, the results showed that for this microphone diaphragm size, the sound power attenuation does not change, i.e., the same results were obtained as when the point error sensors were used in the model. The control system simulation created a node in the pressure across the center of the microphone with positive and negative pressure on either side of the node. The result suggests that the size of the diaphragm is not as critical in the control system as is the location of the acoustic center of the microphone.

The last aspect of the error sensor sensitivity that was investigated was sensitivity to extraneous noise in the error signals. This noise could come from either electrical noise associated with the measurement hardware or acoustical noise at the error sensor. The noise is added to the system at the error microphones in the form of

$$n = Ae^{-j2\pi b}, \tag{17}$$

where A is an amplitude term which can be varied to yield different signal to noise ratios and b is a random number with a uniform distribution to give the noise a random phase element. Thus, the pressure at each microphone, as given in Eqn. (12), was modified to include a noise vector, whose elements are representative of the noise for each error microphone as given in Eqn. (17), given by,

$$\bar{\boldsymbol{P}} = \bar{\boldsymbol{G}}_{cc}\,\bar{\boldsymbol{Q}}_c + \bar{\boldsymbol{G}}_{pp}\,\bar{\boldsymbol{Q}}_p + \bar{\boldsymbol{n}}. \tag{18}$$

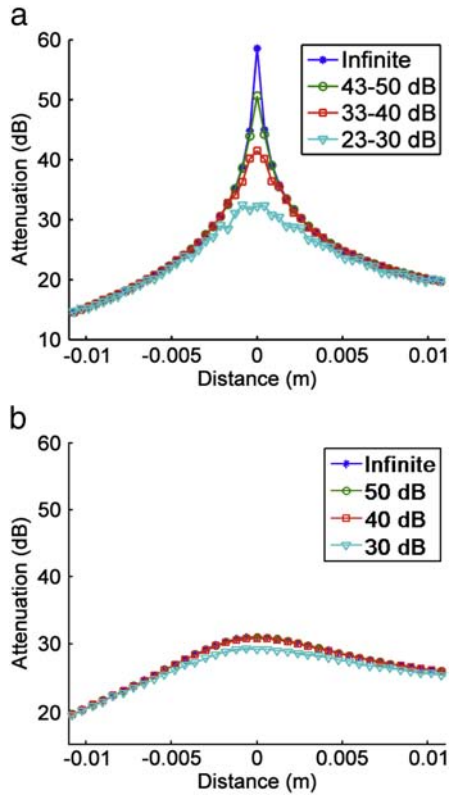

Fig. 6—The predicted sound power attenuation of a primary source with noise added to the error microphones at different signal to noise ratios. Three of the four microphones remain in the optimal locations with one microphone being incremented along the path shown in Fig. 3. a) Attenuation for the linear configuration, with the legend values showing the signal to noise ratio at the far and near microphones. b) Attenuation for the symmetric configuration.

Following the same procedure outlined above of minimizing the squared pressure at each of the microphones results in the control source strengths being given by,

$$\overline{\boldsymbol{Q}}_c = -\left(\overline{\boldsymbol{G}}_{cc}^H \overline{\boldsymbol{G}}_{cc}\right)^{-1}\left(\overline{\boldsymbol{G}}_{cc}^H \overline{\boldsymbol{G}}_{pp}\, \overline{\boldsymbol{Q}}_p + \overline{\boldsymbol{G}}_{cc}^H \bar{\boldsymbol{n}}\right). \quad (19)$$

Equation (19) shows that when the noise is added at the error sensor, it is filtered by the Hermitian transpose of the control source transfer function from the control sources to the microphones. The control source strength from Eqn. (19) was then inserted into the equation for the total sound power of the system, Eqn. (5), in order to determine the attenuation of the primary source sound power. Since the noise is considered to be random, the effect of different signal to noise ratios on the control system is found by running the simulation 100 times with random added noise and finding the resulting average sound power attenuation. For this simulation, the microphones were still incremented through the paths shown in Fig. 3 for the symmetric microphone and the near microphone, leaving out the far microphone. The signal to noise ratios were calculated by finding the pressure at each microphone from the primary source compared to the response from the added noise. The results are shown in Fig. 6 for several signal to noise ratios. As shown, the noise in the control system has a much greater effect on the linear configuration. The attenuation dropped from 59 dB for an infinite signal to noise ratio to 41 dB for a 40 dB signal to noise ratio. Looking at the symmetric configuration, there is virtually no drop for the symmetric case with the same 40 dB signal to noise ratio. Looking further into the linear array case, the control configuration is more sensitive to the noise when the microphone is closer to the optimal location (close to zero on the abscissa).

The overall results show the linear array control system configuration was more sensitive to uncorrelated noise sources compared to the symmetric control system configuration. Additionally, the linear array control configuration is much more sensitive to errors in microphone placement than the symmetric configuration.

4 EXPERIMENTS

4.1 Experimental Setup

The microphone placement sensitivity of the two configurations was then tested experimentally. The primary source used was a 2.5 cm tweeter loudspeaker placed in a speaker plate. The 2.5 cm control sources were placed around the primary source according to Fig. 2 for both configurations. The control set up is shown in Fig. 7. (Only 4 of the 6 control speakers were operated for any given test, to correspond to either the

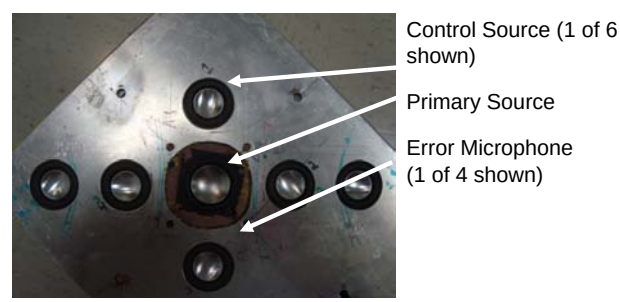

Fig. 7—The experimental setup of the linear array and symmetric configuration used.

linear or symmetric configuration.) The feed-forward control system is implemented using the filtered-*x* LMS algorithm running on a Texas Instruments 320C6713 DSP with a sampling frequency of 4000 Hz. The multi-channel filtered-*x* LMS controller used 20 control filter coefficients and 20 secondary path model coefficients for each filter implemented, with a total of 4 control filters and 16 secondary path model filters. The four control sources were each driven by their own unique control signals, which after adaptation corresponded to the signals that resulted in minimum pressure response at the four microphone error sensors. The sixteen secondary path filters modeled the transfer functions from each of the four control sources to each of the four error sensors. For this work, the secondary path filters were obtained *a priori* using broadband noise excitation of the control sources to obtain the filters. A single reference signal obtained from the input signal to the primary source was used as the reference input for the control system. The error microphones were 6 mm Hosiden electret microphones. Anti-aliasing low-pass filters were implemented using Krohn-Hite 3384 8 pole filters set with a cutoff frequency of 1800 Hz.

The primary source speaker was driven at 600 Hz. This frequency was chosen since the application of interest for this research was the active control of small axial fans, where the blade passage frequency is often close to 600 Hz. The sensitivity of the control system to microphone location was found by placing three of the four microphones in the calculated optimal locations. Following the control paths in Fig. 3, the fourth microphone was incremented at 2.5 mm increments with a total of 9 measurements. Each error microphone path was tested four times. For each of these error sensor locations, the sound power attenuation of the primary field was measured. The sound power measurement was obtained using a rotating semicircular microphone array with a radius of 1.8 m and thirteen 12.7 mm GRAS type I microphones equally spaced along the semicircle. The control set up was placed directly under the center microphone of the array and the array was rotated about the center microphone at 15 degree increments to create a 360 degree hemispherical scan. At each of the measurement microphone locations, the autospectrum was calculated using 15 averages and a frequency resolution of 6.1 Hz. The sound power was then calculated using an area weighting function used by Leishman et al[22]. In this method, an area weighting function is used on the individual microphone measurements to account for the unequal areas swept out by the measurement array to determine the sound power.

To experimentally test whether the error sensor surface area has any impact on performance, control was also run using 12.7 mm type I Larson Davis microphones for the error sensors in place of the 6 mm electret microphones. The larger microphones were placed in the maximum attenuation locations for this trial.

4.2 Results

The results for the four separate trials to measure sensitivity to error sensor placement are shown in Fig. 8. The experimental trials are plotted along with the simulated range for possible attenuations calculated in Fig. 5. Generally the values are within the range predicted by Fig. 5. However, toward the optimal position placement of the moved microphone, the values become closer to the minimum predicted attenuation. With respect to the linear array configuration plots, the far microphone has experimental values that are higher than predicted on the outside tails of the plot. However, the trends for the experimental trials for the far microphone still appear reasonable, with the attenuation sloping downward faster as the microphone moves from the optimal location toward the primary source than when the microphone is moving away from the primary source. This pattern matches the pattern of the simulation shown in Fig. 4 when 3 of the 4 microphones are in the optimal locations. Allowing for an experimental error of up to 1 mm for all four microphones, the data matches what could be reasonably expected from the control system, meaning that most of the data are within the expected range calculated and shown in Fig. 5. The experimental results showed that the linear array does have a significantly greater sensitivity to microphone placement compared to the symmetric array. Looking specifically across the 9 measurements for a single trial (moving one microphone 2 cm) the range of sound power attenuation values for the closer microphone in the linear array configuration was 15–34 dB. This 19 dB range was much higher than the symmetric configuration that had a range of 8 dB (20–28 dB). Specifically, moving off the optimal location in either direction 2.5 mm meant an average of 5.5 dB reduced attenuation for the closer microphone in the linear array configuration, compared to 0.6 dB reduced attenuation for the symmetric configuration.

The error sensor signal to noise ratio is determined by taking a measurement with the control on and off. The signal to noise ratio was determined to be 50–70 dB for the four microphones. The noise simulation plots show that a signal to noise ratio of 50–70 did not have a significant impact on either control configuration. The signal to noise ratio measurement and the experimental results from moving one microphone suggest that microphone placement is the most

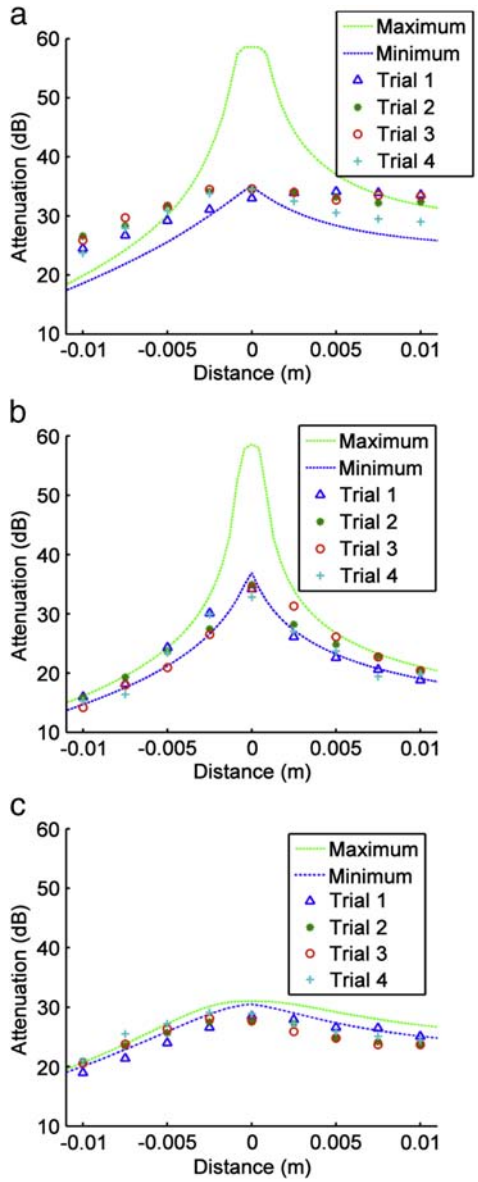

Fig. 8—The experimental results from four experimental runs plotted against the maximum and minimum attenuations of the primary source calculated in Fig. 5 for the a) linear configuration moving a microphone furthest from the primary source b) linear configuration moving a microphone that is closer to the primary source c) symmetric configuration moving a microphone.

important factor in determining the maximum achievable sound power attenuation for this configuration.

When 12.7 mm microphones were used as error sensors for the linear array configuration, the amount of control achieved matched that achieved with 6 mm microphones — 33 dB sound power reduction. The result of 33 dB attenuation using the larger diaphragm microphones as error sensors confirms the simulation result that microphone diaphragm size does not affect the control significantly at this frequency.

5 CONCLUSIONS

The purpose of this paper was to investigate the sensitivity of two different control configurations with regard to error microphone position errors, as well as the sensitivity of the control systems to added noise. The two control systems simulated were a symmetric four control source configuration that surrounded the primary source and a linear array of four control sources with the primary source in the center of the array. The control systems were modeled using baffled free space Green's functions as the transfer function between the sources (primary and control) and the microphones. Simulations were performed using this model. The simulated results showed that the linear array configuration has more sensitivity than the symmetric array configuration with regard to error sensor placement and to extraneous noise sources. A 2.5 mm change in microphone position resulted in a 25–30 dB theoretical loss in attenuation for the linear case, compared to a 2 dB loss for the symmetric case. For the extraneous noise simulation, adding noise to the simulation greatly affected the linear case, with only a minimal effect for the symmetric configuration. A 40 dB signal to noise ratio resulted in a decrease in attenuation from 59 to 41 dB for the linear array configuration.

The experimental results confirmed that the linear array configuration was more sensitive to microphone placement with large decreases in attenuation based on microphone placement error. A 2.5 mm change in the position of a single microphone can cause an average 5.5 dB loss in sound power attenuation for the linear array configuration compared to an average loss of 0.6 dB for the symmetric case. A measurement of the signal to noise ratios at the error microphones showed that in this experimental configuration, extraneous noise was not a significant factor for the control systems. The acoustic center of the microphone proved to be much more important than the size of the microphone, because microphone diaphragm size did not affect the global control results both theoretically and experimentally. Overall, the results show that the control configuration can have a significant impact on the robust nature of the control system, particularly for the linear configuration which exhibited significant sensitivity to microphone placement errors.

6 REFERENCES

1. D.A. Quinlan, "Application of active control to axial flow fans", *Noise Control Engr. J.*, **39**, 95–101, (1992).

2. J. Wang, L. Huang and L. Cheng, "A study of active tonal noise control for a small axial flow fan", *J. Acoust. Soc. Am.*, **117**, 734–743, (2004).
3. A. Gérard, A. Berry and P. Masson, "Control of tonal noise from subsonic axial fan. Part 2: active control simulations and experiments in free field", *J. Sound Vibr.*, **288**, 1077–1104, (2005).
4. J. Wang and L. Huang, "Active control of drag noise from a small axial flow fan", *J. Acoust. Soc. Am.*, **120**, 192–203, (2006).
5. K.L. Gee and S.D. Sommerfeldt, "Application of theoretical modeling to multichannel active control of cooling fan noise", *J. Acoust. Soc. Am.*, **115**, 228–236, (2004).
6. K.L. Gee and S.D. Sommerfeldt, "A compact active control implementation for axial cooling fan noise", *Noise Control Engr. J.*, **51**, 325–334, (2003).
7. B.B. Monson, S.D. Sommerfeldt and K.L. Gee, "Improving compactness for active noise control of a small axial cooling fan", *Noise Control Engr. J.*, **55**, 397–407, (2007).
8. G.C. Lauchle, J.R. MacGillivray and D.C. Swanson, "Active control of axial-flow fan noise", *J. Acoust. Soc. Am.*, **101**, 341–349, (1997).
9. P.A. Nelson, A.R.D. Curtis, S.J. Elliott and A.J. Bullmore, "The minimum power output of free field point sources and the active control of sound", *J. Sound Vibr.*, **116**, 397–414, (1987).
10. S.J. Elliott, P. Joseph, P.A. Nelson and M.E. Johnson, "Power output minimization and power absorption in the active control of sound", *J. Acoust. Soc. Am.*, **90**, 2501–2512, (1991).
11. B.M. Shafer, K.L. Gee and S.D. Sommerfeldt, "Verification of a near-field error sensor placement method in active control of compact noise sources", *J. Acoust. Soc. Am.*, **127**, EL66–EL72, (2010).
12. R.L. Clark and C.R. Fuller, "Optimal placement of piezoelectric actuators and polyvinylidene fluoride error sensors in active structural acoustic control approaches", *J. Acoust. Soc. Am.*, **92**, 1521–1533, (1992).
13. A.P. Berkhoff, "Optimum sensor–actuator distance for decentralized acoustic control", *J. Acoust. Soc. Am.*, **110**, 260–266, (2001).
14. S. Pulthasthan and H.R. Pota. "The optimal placement of actuator and sensor for active noise control of sound–structure interaction systems", *Smart Mater. Struct.*, **17**, 037001, (2008).
15. B.T. Wang, "Optimal placement of microphones and piezoelectric transducer actuators for far-field sound radiation control", *J. Acoust. Soc. Am.*, **99**, 2975–2984, (1996).
16. C.R. Duke, S.D. Sommerfeldt, K.L. Gee and C.V. Duke, "Optimization of control source locations in free-field active noise control using a genetic algorithm", *Noise Control Engr. J.*, **57**, 221–231, (2009).
17. D.A. Manolas, I. Borchers and D.T. Tsahalis, "Simultaneous optimization of the sensor and actuator positions for an active noise and/or vibration control system using genetic algorithms, applied in a Dornier aircraft", *Eng. Comput.*, **17**, 620–630, (2000).
18. H.Y. Guo, L. Zhang, L.L. Zhang, and J.X. Zhou, "Optimal placement of sensors for structural health monitoring using improved genetic algorithms", *Smart Mater. Struct.*, **13**, 528–534, (2004).
19. S. Pottie and D. Botteldooren, "Optimal placement of secondary sources for active noise control using a genetic algorithm", *InterNoise96*, (1996).
20. C.H. Hansen and S.D. Snyder, *Active Control of Noise and Vibration*, E&FN Spon, London, (1997).
21. P.A. Nelson and S.J. Elliot, *Active Control of Sound*, Academic, London, (1992).
22. T.W. Leishman, S. Rollins and H.M. Smith, "An experimental evaluation of regular polyhedron loudspeakers as omnidirectional sources of sound", *J. Acoust. Soc. Am.*, **120**, 1411–1422, (2006).